XL CILAMCE
IBERO-LATIN AMERICAN CONGRESS ON COMPUTATIONAL METHODS IN ENGINEERING
NOVEMBER 11-14, 2019
Praiamar Natal Hotel & Convention Natal, RN-BRAZIL

DETERMINATION OF RELATIVE PERMEABILITY CURVES IN DIGITAL ROCKS AS FUNCTION OF INITIAL SATURATION USING LATTICE-BOLTZMANN METHOD

Carlise Ghisleni
Diogo Nardelli Siebert
Fabiano Gilberto Wolf
Luís Orlando Emerich dos Santos
carlise.ghisleni@posgrad.ufsc.br
diogo.siebert@ufsc.br
fabiano.wolf@ufsc.br
luis.emerich@ufsc.br
Porous Media Research Group (PORO), Technological Center of Joinville, Federal University of Santa Catarina
Street Dona Francisca - 8300, 89.219-600, Joinville/SC, Brazil
Rodrigo Surmas
Leopoldo Américo Miguez de Mello Research and Development Center (CENPES/Petrobras)
Avenue Horácio Macedo - 950, 21941-598, Rio de Janeiro/RJ, Brazil

Abstract. The characterization of fluids in a porous media has attracted interest both academic research and in engineering. Particularly, the comprehension of fluid displacement in a two-phase system affects areas as, enhanced oil recovery, geological carbon dioxide sequestration and contaminated groundwater remediation. To properly characterize multiphase fluid transport in porous media it is necessary to consider a set of properties that exerts influence in the subsurface flow like wettabillity, capillary pressure, viscosity and initial saturation. In this work, we aim to establish a correlation between initial saturation and relative permeability. The later is a key to estimate two-phase flow in petroleum reservoirs because it represents the mobility of one phase in a multiphase saturated porous media. There are many ways to distribute the initial saturation in a porous media. The most common is to randomly allocate the fluids in porous space. Although easily computational implementation, it has no relation with initial distribution expected both from experiments and from natural migration inside reservoirs rocks. To solve this inconsistency, some approaches can be applied: (i) Using gravitational and oscillatory forces to induce separation in an initially random saturated media; (ii) performing forced-drainage and forced-imbibition processes; (iii) allocating the wetting phase next to the solid walls and (iv) filling the smaller pores with wetting phase. In this work we quantify how relative permeability curves respond to the initial condition (i) e (iii) using the color gradient Lattice-Boltzmann Model to simulate relative permeability curves in a two-dimensional porous medium image obtained previously by Sheppard et al. [1]. It was possible to see that random saturation implied in relative permeability deviations due the lack of control in filling porous medium. To EDT, it was also observed some deviations because the nature of algorithm that used random saturation to avoid tendentiousness in filling some porous. The deviations were less apparent in wetting phase than in non-wetting phase. Also, it was observed increase in relative permeability to lower contact angles due the lubrication effect, both, to random and EDT cases.

Keywords: Relative permeability, Initial Saturation, LBM, Spencer's Model, Sandrock, X-ray computed microtomography, Digital petrophysics.

1 Introduction

Characterization of fluid transport in porous medium has great importance in many areas in science and engineering such as enhanced recovery of oil, capture and imprisonment of carbon dioxide, remediation of non-aqueous liquid phases, remediation and transport of contaminants in aquifers and many other [2–4].

Relative permeability is one of the key parameters for describing fluid flow in porous media. It can be interpreted as a property related to mobility of one phase in a multiphase flow [5]. However, relative permeability depends on many flow parameters such as phase saturation, viscosity ratio, motive force and wettability [6].

There are two main ways of experimentally measuring this quantity, the steady-state and transient methods. However, laboratory tests are time-consuming. Thus, several studies have been conducted using the Lattice-Boltzmann Method (LBM), which is able to simulate a wide variety of fluid flow problems in different geometries, both in single-phase and multiphase conditions [7]. The basic premise of LBM is to apply Boltzmann's Transport Equation (LBE), a numerical version of the Boltzmann Equation, to simulate flow in a discrete domain by modeling fluid motion through the evolution od a particle distribution function [8].

Ramstad et al. [9] explored the relative permeability behavior using LBM to reproduce the steady-state and transient experiments in Berea and Bentheimer samples. Results were compared with the experimental results of Øren et al. [10] and Oak et al. [11] for steady-state regime. They noticed that there was low adherence between the simulated drainage curve in a transient regime comparing to the experimental curve. This could be explained by existence of viscous instabilities which violate the darcy's law for two fluids. Understanding the need for visco-capillary approach, Alpak et al. [12] used the LBM based on the free energy model with the visco-capillary coupling to study the topology of the fluid phases, especially the non-wetting phase. This choice was supported by Berg et al. [13] and Liu et al. [14] since relative permeability has a strong correlation with connectivity and, therefore, analyzing non-wetting phase could generate better validations.

Also, other authors studied the behaviour of relative permeability curves: Dou and Zhou [15] analyzed the effect of porous medium heterogeneity in relative permeability results; Zhang et al. [16] studied how changes in geometric characteristics, such as porosity and connectivity, could influence the non-wetting relative permeability curve; Shi and Tang [6] studied the effect of wettability, saturation, porosity and grain distribution and; Li et al. [17] focused on the influence of the wettability and adhesive forces in relative permeability. In these studies, with exception of Zhao et al. [18], only artificial porous media composed of circles, ellipses, squares or spheres were used.

It was also important to point out that, these works computed the relative permeability curves by considering the non-wetting phase randomly distributed inside porous space [9, 15, 16, 19]. However, such a procedure may generate inconsistency in the results, since, when randomly distributed, the non-wetting phase may be inconsistent with the behaviour expected both from fluid migration on nature and from laboratory experiments.

Jiang and Tsuji [20] also agreed with inefficiency of a random saturated porous media. These authors mentioned two main problems associated with this practice: lack of pore filling control and impossibility of considering hysteresis of drainage and soaking processes, which according to Oak et al. [11] directly affects relative permeability curves.

It is worth mentioning that these precautions with initial saturation were received attention in recent works, especially using fluid repositioning by gravitational or oscillatory forces [6, 17, 20] or by attempting to reproduce reservoir conditions [12]. However, these authors did not presented an in-depth analysis of the effects of using these different approaches.

Shi and Tang [6] used a three-dimensional domain to investigate immiscible two-phase flow. The initial saturation consists on wetting phase touching the solid and non-wetting phase occupying the center of porous medium. Then these phases were redistributed by a driving force.

Also, Jiang and Tsuji [20] estimated the relative permeability in a three-phase (water-oil-CO_2)

saturated porous medium. In this case, water and oil were randomly distributed and an oscillatory body force was applied and then CO_2 was injected. In contrast, Alpak et al. [12] sought to reproduce what is observed in laboratory, first performing a forced drainage process to obtain the irreducible saturation and, then, reproducing a forced imbibition.

It can be noted that, among all this studies, none of them explored how the initial saturation behavior of the porous medium can interfere in the relative permeability curves. In this sense, the aim of this work is to study how different initial fluid saturation distributions in porous medium can affect the relative permeability.

This study uses the lattice-Boltzmann Method for multiple immiscible fluids developed by Spencer et al. [21]. The domain is a two-dimension digital image of a sandstone obtained by Sheppard et al. [1] using X-Ray microtomography. The simulations setup used here intends to model a steady state relative permeability experiment. For the initial saturation distribution, two different approaches are analyzed: random distribution of fluids and wetting fluid placing near the solid walls.

2 Lattice-Boltzmann Method

The Lattice Boltzmann Method (LBM) has experienced a fast pace development in the last two decades and has become a novel and powerful computational fluid dynamics (CFD) tool. LBM is particularly successful in applications involving interfacial dynamics and fluid flow through complex geometries [7, 22].

The dynamics of LBM is simple and governed by two steps: collision and streaming. In this method the fluid state in a given point or node is described by the particle distribution functions (PDF), $f_i(\boldsymbol{r}, t)$, which represents the amount of fluid particles in a specific note at the $\boldsymbol{r}$ position in given instant of time t with velocity $\boldsymbol{c_i}$.

As two fluids are being considered, it is necessary to define two PDF's, one for red and other for blue fluid. Following Spencer et al. [21]:

$$f_i(\boldsymbol{r}, t) = R_i(\boldsymbol{r}, t) + B_i(\boldsymbol{r}, t), \tag{1}$$

where $R_i(\boldsymbol{r}, t)$ and $B_i(\boldsymbol{r}, t)$ are colored distribution functions associated to red and blue fluid respectively.

In streaming step, the particles propagate to neighboring lattice nodes in accordance with the pre-established velocity vectors $\boldsymbol{c_i}$ [9]. After this step, the particles located in the same node collide and consequently the local particle distribution function f_i is redistributed to model this process.

To compute collision in all domain it is used two relaxation time (TRT) model, as proposed by Ginzburg [23]. Briefly, this model relay on concept of distribution function decomposition in a symmetric and an antisymmetric part, where, to perform collision, the BGK operator is applied for each part:

$$f_{s,i} = \frac{f_i + f_{-i}}{2}, \tag{2}$$

$$f_{\alpha,i} = \frac{f_i - f_{-i}}{2}, \tag{3}$$

$$f_i' = \frac{f_{s,i} + f_{s,i}^{eq}}{\tau_s} + \frac{f_{\alpha,i} - f_{\alpha,i}^{eq}}{\tau_\alpha}, \tag{4}$$

here, τ correspond to relaxation time of distribution function where α is related to antisymmetric part and s to symmetric part. Also f_i^{eq} is the distribution function in equilibrium, correlated with symmetric and antisymmetric parts, which is given by:

$$f_i^{eq}(\boldsymbol{r}, t) = \rho\omega i \left(1 + \frac{c_{i,\alpha}u_\alpha}{c_s^2} + \frac{c_{i,\alpha}c_{i,\beta} - c_s^2\delta_{\alpha,\beta}}{2c_s^4}u_\alpha u_\beta\right), \tag{5}$$

where c_s is a function of lattice net whose value is $1/\sqrt{3}$.

Aditionally, an external force can be considered by adding momentum during the collision process. In Spencer et al. [21], the colour-blind PDF undergoes a collision rule with a source force term F_i:

$$f_i^* = f_i^{'} + F_i. \tag{6}$$

This variable, F_i, is related to the effect of Laplace pressure step across interface, which is proportional to fluids' interfacial tension and mean radius curvature. Therefore, the force term due to interfacial tension is computed by:

$$F_i(\boldsymbol{r}, t) = \rho\omega i \left(\frac{\alpha|\nabla\omega_r|}{c_s^2}\right)(n_\alpha n_\beta - \delta_{\alpha,\beta})(c_{i,\alpha}c_{i,\beta} - c_s^2\delta_{\alpha,\beta}), \tag{7}$$

The local concentration gradient can be calculated by,

$$\nabla\omega_r = \sum_i \omega_r(\boldsymbol{r} + \boldsymbol{c_i})\boldsymbol{c_i}, \tag{8}$$

where ω_r is the local red fluid concentration. It has been shown by Lishchuk et al. [25] and Halliday et al. [26] that, phase field when appropriately evolved and coupled to an immersed boundary or interface inducing force can recover correct dynamics for continuum regime and kinematics.

The normal vector to an interface region can be defined from equation:

$$\widehat{n} = -\frac{\nabla\omega_r}{|\nabla\omega_r|}. \tag{9}$$

and the force term associated to surface tension from:

$$\gamma = 2\rho c_s^2\alpha. \tag{10}$$

Besides collision and propagation the model of Spencer et al. [21], includes also a recoloring step, first introduced by Rothman and Keller [24]. In this step, the two colored distribution functions are reconstructed individually by the following equations:

$$B_i(\boldsymbol{r}, t) = \omega_b f_i - \omega i\beta\rho\omega_r\omega_b(\widehat{n}.\boldsymbol{c_i}), \tag{11}$$

$$R_i(\boldsymbol{r}, t) = \omega_r f_i - \omega i\beta\rho\omega_r\omega_b(\widehat{n}.\boldsymbol{c_i}), \tag{12}$$

According to Spencer et al. [21], the nodal density of red and blue fluids can be computed by,

$$\rho_R(\boldsymbol{r}, t) = \sum_i R_i(\boldsymbol{r}, t), \tag{13}$$

$$\rho_B(\boldsymbol{r}, t) = \sum_i B_i(\boldsymbol{r}, t). \tag{14}$$

The steaming step is updated according the equations:

$$B_i(\boldsymbol{r} + \boldsymbol{c_i}, t + 1) = B_i(\boldsymbol{r}, t), \tag{15}$$

$$R_i(\boldsymbol{r} + \boldsymbol{c_i}, t + 1) = R_i(\boldsymbol{r}, t). \tag{16}$$

In this problem, sample's relative permeability is measured using a reflected geometry. Reflection may be done in the same axis which relative permeability will be measured. The value of its property is defined by:

$$k_{ri} = \frac{k_i}{k}. \tag{17}$$

It is valuable to reinforce that geometry must be periodic to avoid inconsistencies at boundaries. According to Guo and Shu [27] it is important to emphasize the importance of initial and boundary conditions in fluid dynamics since they are essential in determination of flow solution. Generally, these conditions have significant influences on accuracy, stability and convergence of LBE. For agreeing with Guo and Shu [27] this article investigates the behaviour of relative permeability curves as function of initial saturation.

3 Results and Discussion

To initiate simulations, the first need was to define the geometry which would be used. The chosen porous medium was previously obtained by Sheppard et al. [1] using X-ray microtomography from an unconsolidated sandstone, as seen in Figure 1.

Figure 1. Porous medium from inconsolidated sandstone.

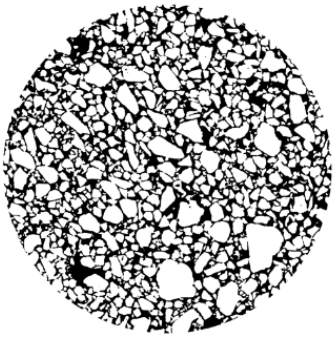

This image was cut in rectangular shape and then eroded to achieve higher porosity. The initial image had porosity equal to 37.821%, while final image has 67.696%. This handling was needed because there was no connectivity in the original rock for low non-wetting phase initial saturation. Image was also mirrored to create geometry continuity, where the result can be seen in Figure 2. It was also defined that rock surface is water-wetting and the oil is non-wetting fluid.

Figure 2. Modified porous medium to increase porosity.

In simulations, contact angle was given by:

$$\theta = arccos(2w_{wall} - 1). \tag{18}$$

The chosen contact angles were 78.47° and 66.42°, when w_{wall} was equal to 0.4 and 0.3, respectively. There was no flow pressure gradients and imposed pressure was equal to $0.1Darcy$.

To begin LBM simulations, two algorithms were developed to saturate the geometry showed in Figure 2: one to random saturate and other to saturate based on exact Euclidian Distance Transform (EDT).

According to Lucet [28], EDT method computes a new image in which the value at each pixel is equal to the Euclidean distance from that pixel to the background. Thought this method it is possible to allocate the initial saturation of wetting phase next to the solid walls. Figure 3 shows the difference between (a) random and (b) EDT method for 40% non-wetting fluid.

Figure 3. Initial saturation based on different methods.

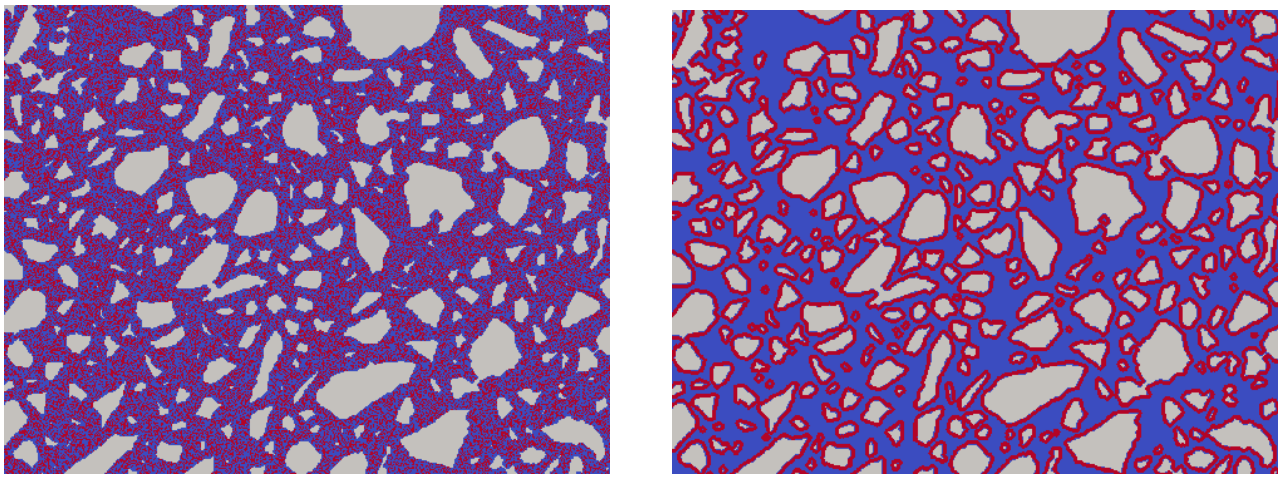

(a) Randomly saturated

(b) Saturated by EDT method

After defining initial saturation, LBM simulations were carried out until achieve steady-state flow. Figure 4 shows the behaviour observed in relative permeability curves for (a) random and (b) EDT initial saturation.

Figure 4. Relative permeability curves considering different initial saturation methods.

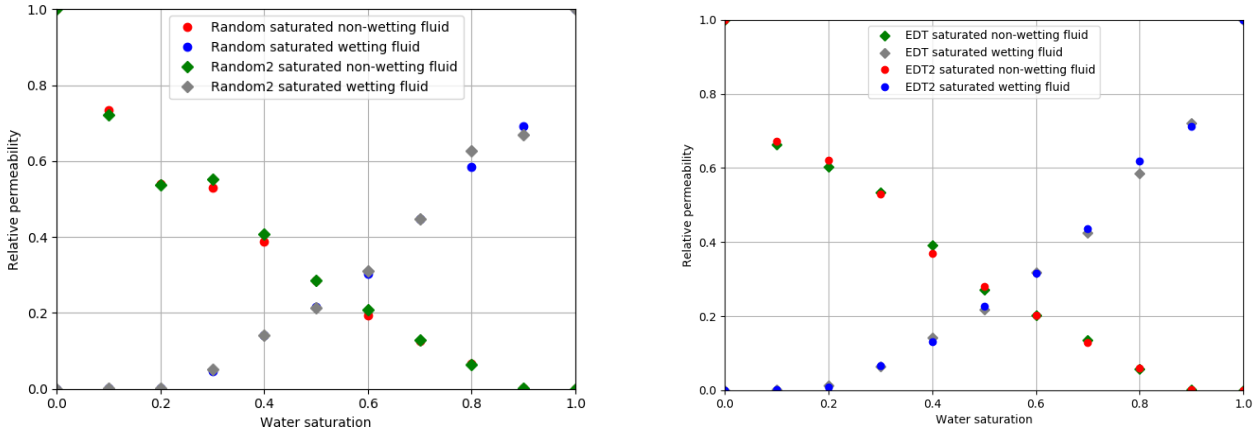

(a) Randomic saturated relative permeability curves

(b) EDT saturated relative permeability curves

It was possible to note that curves followed same trend, but some values deviated from first to second set of simulations. Deviations were less significant in wetting phase than in non-wetting phase. Also, random initial saturation presented fewer adherence when compared to EDT.

The results corroborate to conclude that, when utilizing random initial saturation, relative permeability curves cannot be predicted. It is due the lack of control in filling porous medium. To each new random saturation, voids will be filled in aleatory way, so, it is not possible to predict which porous might contain wetting or non-wetting fluid.

To EDT method, the results in relative permeability showed fewer deviations, but it still apparent in results. It can be explained due the way initial saturation algorithm was written. It is valid to remember that, the algorithm calculates the number of pores which may be saturated with oil and also, computes the Euclidean distance from that pixel to background. When the number of EDT pixels is grater than the number of sites which may be saturated, the algorithm saturates randomly this remain quota. It is necessary because there are more pixels to fill than fluid. To avoid tendentiousness, it was preferred to use random saturation in this cases.

Regarded behaviour when contact angle was analyzed, Figure 5 shows relative permeability curves for (a) contact angle equal to 78.47° and (b) contact angle equal to 66.42°.

Figure 5. Relative permeability curves for different contact angles.

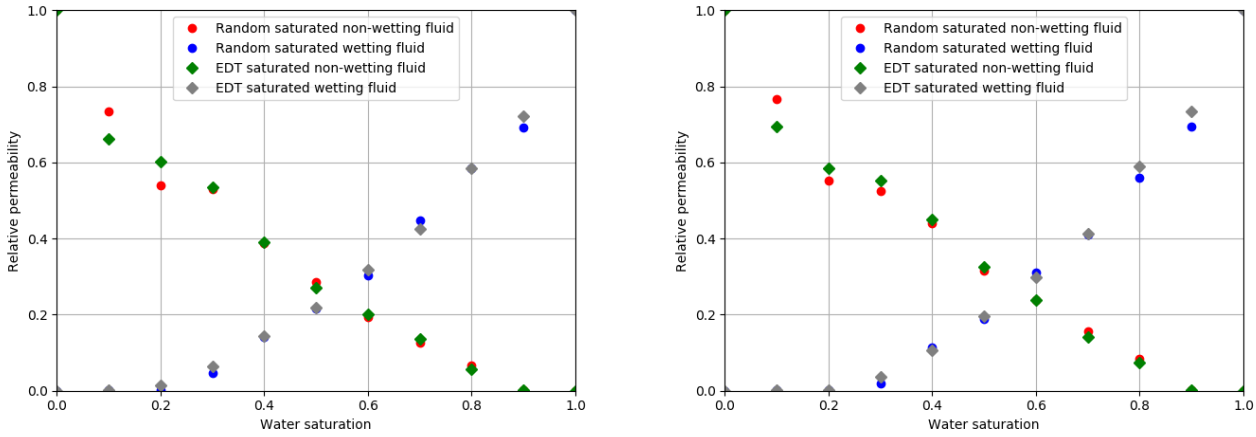

(a) for $\theta = 78.47°$

(b) for $\theta = 66.42°$

It is possible to observe that, when contact angle was equal to 66.42°, values for oil relative permeability were higher than to contact angle equal to 78.47° for both methods, random and EDT. It may be caused due lubrication effect [15, 16, 29] that induces wetting phase to allocate next the walls increasing non-wetting phase mobility. Also, this effect tends to increase frictional forces between wetting phase and rock, incurring in lower wetting phase relative permeability.

4 Conclusion

Following the literature, many authors conducted studies about relative permeability curves in rocks randomly saturated [9, 15, 16, 19]. However, some studies showed that there are two main problems associated with this practice that affects directly the relative permeability: lack of pore control filling and impossibility of considering hysteresis in drainage and soaking processes. However, none articles presented an in-depth study of relative permeability curves as function of initial saturation.

To handle this subject properly, first taken decision was about geometry and the methods which might be used. To likelihood physical rocks, it was chosen to use digital images, where an image obtained by Sheppard et al. [1] using X-Ray microtomography was preferred. However, this image had nonexistent connectivity for low initial saturation what demanded a set of sequential erosion to achieve higher porosity. This step, probably, will not be needed working with tree-dimensional images because there was one more direction to connect the flow.

Regarding method, only two saturation ways were chosen: random and EDT. The first one was preferred to understand the answers obtained in other papers and the second one was chosen as being a more coordinated way to fill the porous medium.

Also, simulations were carried out until reach steady-state. The influence of contact angles in the curves were also studied.

As answers, it was observed that random initial saturation influence relative permeability curves in an unpredictable way. For each random filling, permeability curves suffered deviations. Also, the same behaviour was observed to EDT due the way initial saturation algorithm was written, considering random saturation for remain fluid quota. It was also observed that wetting phase suffered less deviations than non-wetting phase.

For different contact angles, answers were adherent with literature [15, 16, 29]. For lower contact angles, lubrication effect helped non-wetting phase to gain mobility. Also, it incurred in lower wetting

phase mobility due the increasing of frictional force. It is worth to point that this behaviour was observed for even random and EDT methods.

References

[1] Sheppard, A., Arns, C., Sakellariou, S., Senden, T., Sok, R., Avendunk, H., ans A Limaye, M. S., & Knachstedt, M., 2006. Quantitative properties of complex porous materials calculated from x-ray ct images.

[2] Kang, Q., Lichtner, P. C., Viswananthan, H. S., & Abdel-Fatthah, A. I., 2010. Pore scale modeling of reactive transport involved in geologic co2 sequestration. pp. 197–213.

[3] Dai, Z., Middleton, R., Viswanathan, H., Fessenden-Rahn, J., Baumann, J., Pawar, R., Lee, S. Y., & McPherson, B., 2013. An integrated framework for optimizing co2 sequestration and enhanced oil recovery. pp. 49–54.

[4] Chen, L., Kang, Q., Robinson, B. A., He, Y. L., & Tao, W. Q., 2013. Pore-scale modeling of multiphase reactive transport with phase transitions and dissolution-precipitation processes in closed systems.

[5] Lyons, W., 2010. *Working guide to reservoir engineering*, volume 1. Elsevier.

[6] Shi, Y. & Tang, G. H., 2018. Relative permeability of two-phase flow in three-dimensional porous media using lattice boltzmann method. pp. 101–113.

[7] Chen, S. & Doolen, G. D., 1998. Lattice boltzmann method for fluid flows. pp. 329–364.

[8] Apourvari, S. N. & Arns, C. H., 2016. Image-based relative permeability upscaling from the pore scale. pp. 161–175.

[9] Ramstad, T., Idowu, N., & Nardi, C., 2011. Relative permeability calculations from two-phase flow simulations directly on digital images of porous rocks. pp. 487–504.

[10] Øren, P. E., Bakke, S., & Arntzen, O. J., 1998. Extending predictive capabilities to network models. pp. 324–336.

[11] Oak, M. J., Baker, L. E., & Thomas, D. C., 1990. Three-phase relative permeability of berea sandstone.

[12] Alpak, F. O., Berg, S., & Zacharoudiou, I., 2018. Prediction of fluid topology and relative permeability in imbibition in sandstone rock by direct numerical simulation. pp. 49–59.

[13] Berg, S., Rücker, M., Georgiadis, H., Ott, H., der Linde, H. V., Enzmann, F., Kersten, M., Armstrong, R. T., With, S. D., Becker, J., & Wiegmann, A., 2016. Connected pathway relative permeability from pore-scale imaging of imbibition. pp. 24–35.

[14] Liu, Z., Herring, A., Arns, C., Berg, S., & Armstrong, R. T., 2017. Pore-scale characterization of two-phase flow using integral geometry. pp. 99–117.

[15] Dou, Z. & Zhou, Z.-F., 2013. Numerical study of non-uniqueness of the factors influencing relative permeability in heterogeneous porous media by lattice boltzmann method. pp. 23–32.

[16] Zhang, D., Papadikis, K., & Gu, S., 2016. A lattice boltzmann study on the impact of the geometrical properties of porous media on the steady state relative permeabilities on two-phase immiscible flows. pp. 61–79.

[17] Li, Z., ad G Yan, S. G.-T., Scheuermann, A., & Li, L., 2018. A lattice boltzmann investigation of steady-state fluid distribution, capillary pressure and relative permeability of a porous medium: Effects of fluid and geometrical properties. pp. 153–166.

[18] Zhao, H., Ning, Z., Kang, Q., Chen, L., & Zhao, T., 2017. Relative permeability of two immiscible fluids flowing through porous media determined by lattice boltzmann method. pp. 53–61.

[19] Landry, C. J., Karpyn, Z. T., & Ayala, O., 2014. Relative permeability of homogenous-wet and mixed-wet porous media as determined by pore-scale lattice boltzmann modeling. pp. 3672–3689.

[20] Jiang, F. & Tsuji, T., 2016. Estimation of three-phase relative permeability by simulating fluid dynamics directly on rock-microstructure images. pp. 11–32.

[21] Spencer, T. J., Halliday, I., & Cure, C. M., 2010. Lattice boltzmann equation method for multiple immiscible continuum fluids.

[22] Huang, H., Sukop, M., & Lu, Y. X., 2015. *Multiphase Lattice Boltzmann Methods: Theory and application.*, volume 1. John Wiley and Sons.

[23] Ginzburg, I., 2005. Equilibrium-type and link-type lattice boltzmann models for generic advection and anisotropic-dispersion equation. pp. 1171–1195.

[24] Rothman, D. H. & Keller, J. M., 1988. Immiscible cellular-automaton fluids.

[25] Lishchuk, S. V., Halliday, I., & Care, M. C., 2003. Lattice boltzmann algorithm for surface tension with greatly reduced microcurrents.

[26] Halliday, I., Hollis, A. P., & Care, M. C., 2007. Lattice boltzmann algorithm for continuum multi-component flow.

[27] Guo, Z. & Shu, C., 2013. *Lattice Boltzmann Method and Its Applications in Engineering*. World Scientific.

[28] Lucet, Y., 2006. New sequential exact euclidean distance transform algorithms basedon convex analysis.

[29] Goel, G., Abidoye, L. K., Chahar, B. R., & Das, D. B., 2016. Scale dependency of dynamic relative permeability– satuartion curves in relation with fluid viscosity and dynamic capillary pressure effect.